A Comparative Study of CO_2 Heat Pump Performance for Combined Space and Hot Water Heating

Eivind Brodal* and Steve Jackson

UiT-The Arctic University of Norway

Abstract

Heat pumps used for combined space and hot water heating are often used in modern energy-efficient buildings. Performance depends on both system design (exchanger sizes, compressor efficiency, etc.) and operating conditions (inlet water temperature, ratio between space and water heating, etc.). Designs using both CO_2 and HFCs, such as R410A, are available, but the relative performance of these is not extensively studied.

This article presents performance results based on a system model developed in MATLAB where exchangers are modelled using fixed temperature pinches and pressure drops. Ejectors and compressors are modelled using defined efficiencies. Operating parameters are optimized using the Genetic Algorithm for a set of sensitivity studies. The results show that CO_2 can outperform R410A when the ratio of space to water heating is below 0.6 – 1.0, feedwater is below 20 °C (as in norther Europe) and heat exchangers are designed with temperature pinches below 10 K.

Keywords

Integrated heat pump; R744; R410A; Ejector; Optimization; Pinch point

*** Corresponding author. Tel.: +47 77660364. E-mail:** eivind.brodal@uit.no

Nomenclature		**Subscripts**	
COP	Coefficient of performance [-]	comp	Compressor
DHW	Domestic hot water	crit	Critical
HFC	Hydrofluorocarbons	ejec	Ejector
g	Inequality constraints function	is	Isentropic
GWP	Global warming potential	rec	Recovered
h	Specific enthalpy [kJ kg^{-1}]	refrig	Refrigerant
k	Penalty factor		
LMTD	Log mean temperature difference		
LNG	Liquefied natural gas		
$\dot{m}$	Mass flow rate [kg s^{-1}]		
NTU	Number of transfer units		
P	Duty [kW]		
p	Pressure [bar]		
Δp_{ex}	Pressure drop in heat exchangers		
q	Penalty function		
r_{heat}	Heating ratio (Space to DHW heating) [-]		
R_{refrig}	Refrigerant (CO_2 or R410A)		
T	Temperature [°C]		
T_{a}	Temperature at point “a” in Figure 1 [°C]		
$\overline{T}_{\mathrm{evap}}$	Average evaporation temperature [°C]		
$\mathbf{X}$	Key design variables		

$\mathbf{Z}$	Optimized variables
η_{comp}	Isentropic efficiency compressor [%]
η_{ejec}	Ejector efficiency [%]

1 Introduction

Heat pumps used for combined space and domestic hot water (DHW) heating, also known as integrated heat pumps, represent a technology under development, as discussed in the field study report by Stene and Alonso (2016). Integrated heat pumps can be used simultaneously for heating and cooling (Byrne et al., 2009), or designed to operate in reversible mode for space cooling during summer (Minetto et al., 2016), or in large district heating networks (Elmegaard et al., 2016). The history and current status is also discussed in the review articles by Hepbasli and Kalinci (2009) and Arpagaus et al. (2016). Heat pumps are typically compared on energy efficiency and cost, but the refrigerant used is also an important factor. Replacing hydrofluorocarbons (HFCs) with more environmentally friendly alternatives has become compulsory worldwide. This is due to the entry into force of strict legislative acts aimed at environment preservation, such as the EU F-Gas regulation (EU, 2014), which are pushing towards the adoption of refrigerants with low global warming potential (GWP), like CO_2 with a GWP=1. The focus of this study is CO_2, which is also inexpensive, non-flammable, non-toxic, and has other advantages since it operates transcritical and therefore can match the temperature profile of the DHW heating.

Energy efficient CO_2-based processes typically have three gas coolers to match the refrigerant temperature profile in the exchangers with the space and hot water heating (Stene, 2005). Process performance depends on system design and operating conditions, e.g. inlet and outlet water temperatures, exchanger sizes (gas coolers, internal heat exchanger and evaporator), compressor efficiency and the profile of the heating demand. The ratio between space and DHW heating is particularly important for the heating efficiency (Stene, 2007a). Houses constructed according to the Norwegian building code from 1997 are between 2.2 and 3.4 (Stene, 2007a). Buildings with a large showering consumption such as sport centers and hotels often have much lower space heating demand relative to DHW (Stene and Alonso, 2016). Low-energy buildings and passive houses in Norway have annual ratios ranging from 0.40 to 0.85 (Stene, 2007b), and are estimated to increase rapidly from around 3 % in 2014 to 40 % in 2050 (Nord et al., 2016). Another important performance factor is the feedwater temperature, which is related to the city water temperature, but also affected by thermodynamic losses in the DHW tank, caused by mixing of hot and cold water which increases the feedwater temperature (Stene, 2005; Yokoyama et al., 2007). For a large variety of heat pumps, the energy efficiency can be improved if a two-phase ejector for expansion work recovery is included (Stene, 2007a; Banasiak et al., 2012; Banasiak et al., 2015; Pottker and Hrnjak, 2015; Boccardi et al., 2017). Two-phase ejectors in systems with two gas coolers have previously been modelled by Minetto et al. (2016). However, to the best of the authors' knowledge, the benefits of using ejectors in energy efficient integrated heat pumps with three gas coolers have not been studied in detail.

Conventional one-stage integrated heat pump systems are typically based on HFCs, like R410A (GWP = 1924), and operate with one condenser and one desuperheater in subcritical processes (Blanco et al., 2012). The first transcritical integrated heat pump prototypes were introduced by Nekså (2002) and Stene (2005), and where CO_2 (R744) processes with two and three gas coolers, respectively. Heat pumps based on CO_2 have been known for more than two decades to be very efficient for tap water heating (Nekså et al., 1998), but for space heating processes R410A is reported as more efficient than CO_2 Richter et al. (2003). That is, integrated CO_2 heat pumps outperform conventional HFC-based systems if the space heating demand is small compared to the DHW heating demand (Stene, 2007b). However, there is little study work on where the trade-off point is.

To the best of the authors' knowledge, most of the relevant studies have only discussed pure DHW heating or pure space heating, i.e. systems with only one gas cooler or condenser. A few

experimentally based performance studies have been conducted in the past on integrated CO_2 heat pumps (Nekså, 2002; Stene, 2005; Heinz et al., 2010; Minetto et al., 2016; Stene and Alonso, 2016). The data presented in these references is based on a few real operational cases that are all influenced by a large number of parameters related to the actual exchanger designs and sizes. As a result, these studies are not able to discuss sensitivity to important factors in detail. There are only a few theoretical studies modelling integrated heat pumps, and they all model state solutions for fixed systems using different heat exchanger models like the log mean temperature difference (LMTD) and the number of transfer units (NTU) method (Byrne et al., 2009; Blanco et al., 2012; Minetto et al., 2016). Byrne et al. (2009) simulated the annual coefficient of performance (COP) for CO_2 heat pumps with three gas coolers designed for simultaneous heating and cooling. Blanco et al. (2012) modelled integrated heat pumps with one condenser and one desuperheater for subcritical R410A processes. Minetto et al. (2016) studied annual performance of reversible CO_2 heat pumps with two gas coolers and an ejector, created a model based on experimental data and compared the performance with a state-of-the-art R410A unit. Heinz et al. (2010) simulated and conducted experiments on integrated CO_2-based heat pumps for low-heating-energy buildings, and Stene and Alonso (2016) presented a report on field measurements of heat pump systems in net zero energy buildings. These studies show that CO_2 units can be very efficient when the ratio between space and water heating is low, but are inefficient for pure space heating and cooling service.

In this work, the number of design dependent variables are reduced through multivariable optimization, and by modelling the gas coolers using a minimum allowed temperature difference between the two fluids exchanging heat, which is also known as the temperature pinch. Parameters related to heat exchanger sizing, and optimal high pressure control of the backpressure valve set point, disappear as input parameters in the optimized model, which makes this method suitable as a basis in a comparative study of performance. This is a new approach to investigate performance of integrated heat pumps with multiple gas coolers, e.g. used in sensitivity studies of mixed refrigerant liquefied natural gas (LNG) cascade processes (Ding et al., 2017).

To the best of the authors' knowledge, neither the sensitivity to important factors in integrated heat pump systems, nor the performance improvement realizable through the inclusion of an ejector is well documented in earlier literature. The scope of this study is, therefore, to conduct a sensitivity study which describes the situations where CO_2 outperforms conventional HFC-based systems and vice versa, and present process data that can contribute to more efficient system designs and increase our understanding of how the equipment effects the performance.

The methods used in this study are described in Section 2. The results are presented in Section 3, and the discussion in Section 4. The main conclusions from this study are summarized in Section 5.

2 Method

This chapter explains the development of the multivariable optimization model that forms the basis for this study.

2.1 System Design and Performance Modelling

This article studies the integrated heat pump described in Figure 1, using CO_2 or R410A as refrigerant. The design is similar to the CO_2-based prototype investigated by Stene (2005). However, an electrical heater has been included to make the model more general, so that the processes can be optimized for any heating scheme or compressor model. The subcritical R410A systems are assumed to operate similarly to the transcritical CO_2 heat pump, as discussed by Blanco et al. (2012), in order to set up a fair basis for comparing the two refrigerants.

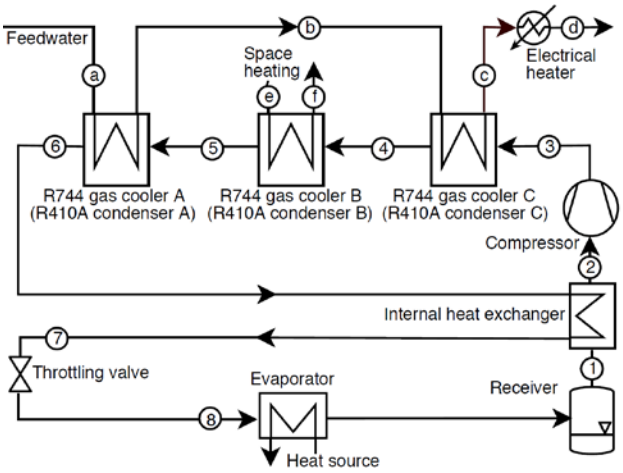

Figure 1. Flow diagram of a combined space and hot water heat pump (ABC).

The process performance is complex, as illustrated by Stene (2005). It depends both on operating conditions, e.g. inlet and outlet water temperatures, the ratio between space and water heating (r_{heat}), the average evaporation temperature ($\bar{T}_{\mathrm{evap}}$), and several system design parameters such as the refrigerant (R_{refrig}), the pressure drop in the exchangers (Δp_{ex}), the temperature pinch in exchangers (T_{pinch}) and the compressor efficiency (η_{comp}).

The models developed here, for both CO_2 and R410A based systems, are based on the assumption that the process is optimized by a control system which adjusts the set pressure of the throttling valve (back pressure valve), i.e. the system is always operating with the most energy efficient R744 gas cooler/R410A condenser pressure (p_3). This is not a standard method for R410A, but neither are the three coolers replacing the conventional condenser in Figure 1. However, in order to build a fair basis for comparison, it was realized during the optimization work that it was necessary to also give R410A systems the opportunity to operate at the most efficient pressure (p_3). The algorithm for calculating enthalpies and the temperature profile in the gas coolers, is based on 14 design parameters:

$$\mathbf{X} = [R_{\mathrm{refrig}}, T_{\mathrm{a}}, T_{\mathrm{d}}, T_{\mathrm{e}}, T_{\mathrm{f}}, \bar{T}_{\mathrm{evap}}, \eta_{\mathrm{comp}}, r_{\mathrm{heat}}, \Delta p_{\mathrm{ex}}, T_2, p_3, h_4, h_5, h_6] \quad (1)$$

where h is specific enthalpy. Figure 2 shows a nearly optimized CO_2-based integrated heat pump process in a logarithmic pressure-enthalpy (ph) diagram, and the corresponding temperature profile in the gas coolers. Figure 3 shows another process with R410A, where condenser A, B and C are operating mostly as a desuperheater, condenser and sub cooler, respectively. However, point 4 and 5 are not necessarily at bubble point or dew point, as illustrated by Figure 3. The different points in these process are calculated from $\mathbf{X}$ using CoolProp (Bell et al., 2014). For CO_2, CoolProp uses a pure fluid equation of state (EOS) introduced by Span and Wagner (1996), which is a "state of the art" property model for CO_2 (Wilhelmsen et al., 2012). R410A is an azeotropic mixture, and is modelled in CoolProp using a pseudo-pure fluid EOS (Lemmon, 2003).

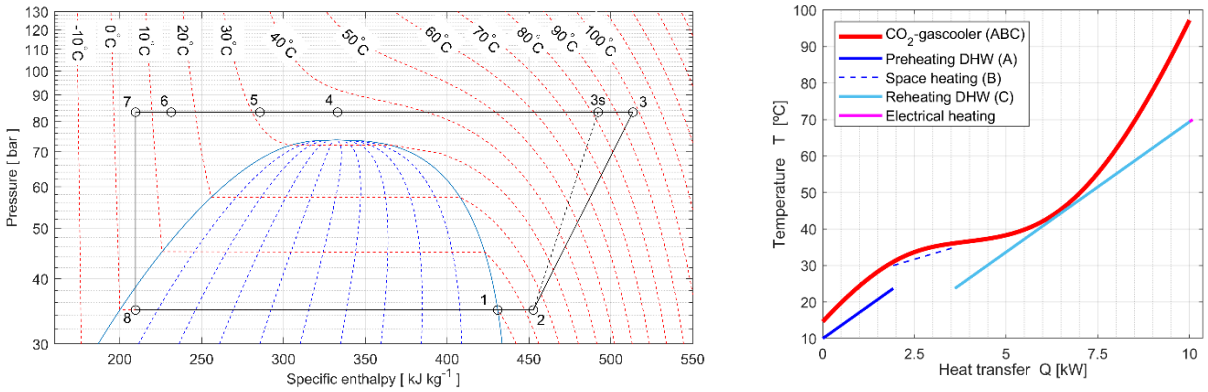

Figure 2. Nearly optimized CO_2 process with Δp_{ex} =0.0 bar, $T_{pinch} \geq 1.0$ K, r_{heat} =0.20, T_a =10 °C, T_d =70 °C, T_e = 35 °C and T_f =30 °C (left). Temperature profile in the gas coolers (right). Fully optimized processes have zero electrical heating.

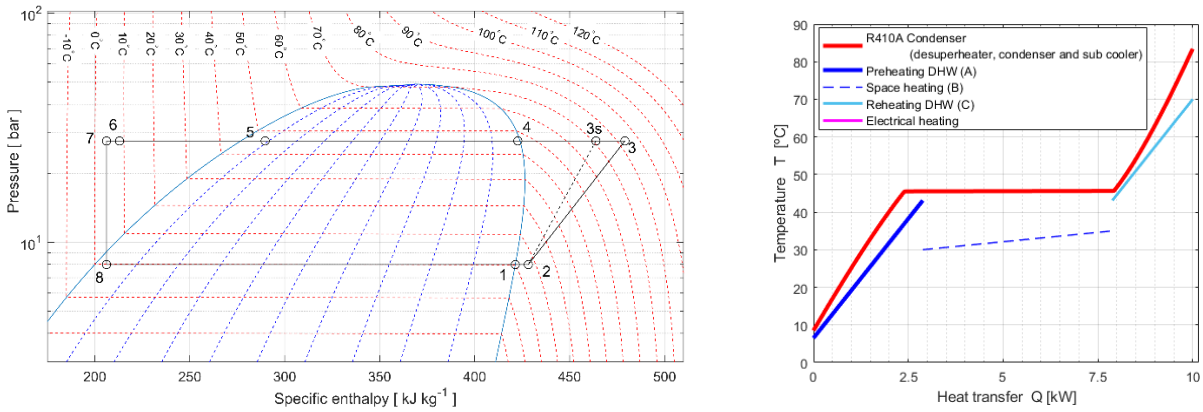

Figure 3. Optimized R410A process with Δp_{ex} =0.0 bar, $T_{pinch} \geq 2.0$ K, r_{heat} =0.50, T_a =6.5 °C, T_d =70 °C, T_e = 35 °C and T_f =30 °C (left). Temperature profile in condenser A, B and C (right).

2.1.1 System Performance

Heat pump systems operating under the same conditions, such as $T_{\mathrm{a}}, T_{\mathrm{d}}, T_{\mathrm{e}}, T_{\mathrm{f}}$ and r_{heat}, can be compared based on their electrical power consummation, e.g. using the coefficient of performance, which can be expressed using the same numbering convention as in Figure 1:

$$\mathrm{COP} = \frac{P_{\mathrm{heat}}}{P_{\mathrm{comp}} + P_{\mathrm{el.heater}}} = \frac{\dot{m}_{\mathrm{a}}(h_{\mathrm{d}} - h_{\mathrm{a}}) + \dot{m}_{\mathrm{e}}(h_{\mathrm{f}} - h_{\mathrm{e}})}{\dot{m}_2(h_3 - h_2) + \dot{m}_{\mathrm{a}}(h_{\mathrm{d}} - h_{\mathrm{c}})} = \frac{\dot{m}_2(h_3 - h_6) + \dot{m}_{\mathrm{a}}(h_{\mathrm{d}} - h_{\mathrm{c}})}{\dot{m}_2(h_3 - h_2) + \dot{m}_{\mathrm{a}}(h_{\mathrm{d}} - h_{\mathrm{c}})} \tag{2}$$

where $\dot{m}$ is mass flow, P_{heat} is the total heating capacity and P_{comp} + $P_{\mathrm{el.heater}}$ is the electrical energy consumption of the compressor plus the electrical heater.

2.1.2 Heat Exchanger Modelling

Several different approaches can be considered for the modelling of the heat exchangers. The approach selected in this study uses a minimum approach temperature in the internal heat exchangers and in all three gas coolers, at each of the operating cases considered. However, the minimum approach temperature T_{pinch} is not treated as a design parameter in **X**, but used as a constraint in the optimization process as described in section 2.2.

The temperature pinch in the internal heat exchanger is located at the end, and is therefore straight forward to compute. In contrast, the temperature profile in the gas coolers has to be modelled, as illustrated in Figure 2, in order to calculate the minimum pinch temperature, which is internal. In the evaporator, the average refrigerant temperature is used to compare cases, i.e. $\bar{T}_{\mathrm{evap}} = (T_1 + T_8)/2$ for the system described in Figure 1. The use of average refrigerant temperature is a simplification used to avoid defining extra heat source parameters, like flow and inlet and outlet temperatures.

Pressure drop directly impacts the performance of the refrigeration loop, as illustrated in Figure 4, and is particularly important when modelling low pressure systems (Blanco et al., 2012). In this study, all heat exchangers (both for CO_2 and R410A) are modelled with fixed pressure drops (Δp_{ex}). Because the COP for a refrigeration loop depends not only on the size of the exchanger pressure drops, but also the pressure drop profile in each exchanger, a linear pressure drop profile has been assumed where $\Delta p \propto P$, where P is the amount of heat transferred in the exchanger. Equation (3) illustrates how the pressure drop profile for 'Gas Cooler C' is calculated.

$$p = p_3 - \Delta p_{ex}\left(\frac{h-h_3}{h_4-h_3}\right) \quad \text{for} \quad h_3 \geq h \geq h_4. \tag{3}$$

2.1.1 Ejector Performance Modelling

The layout of the components between points 7 and 1 are changed if an ejector is included. The ejector system design studied in this article is shown in Figure 4, which also illustrates a CO_2-based process in a logarithmic ph diagram.

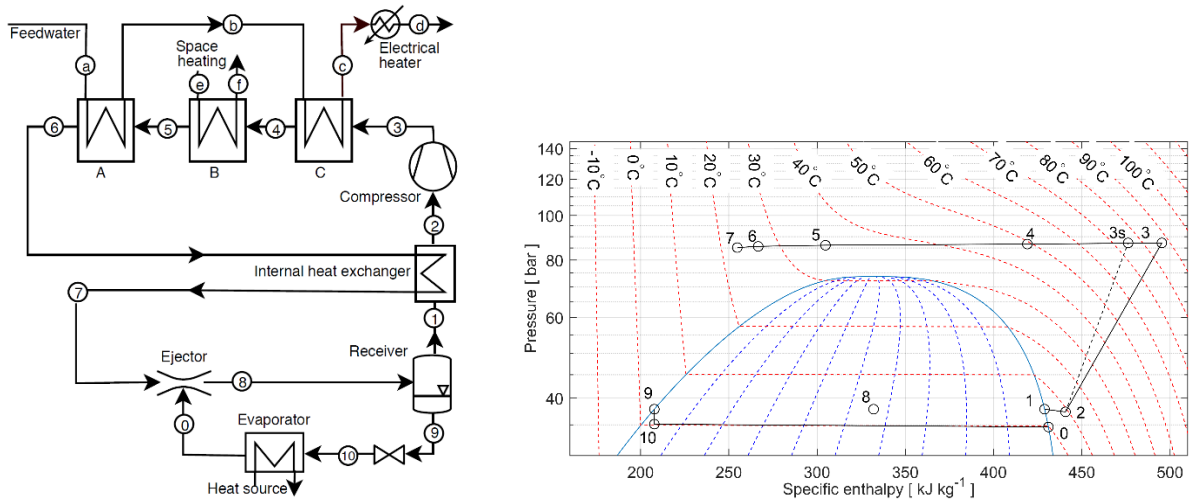

Figure 4. Left: flow diagram of a CO_2 heat pump with an ejector modification (ABC + ejector). Right: example of a CO_2 process with ejector having 35 % efficiency, where all exchangers have 0.5 bar pressure drop.

The performance of the heat pump depends on the efficiency of the ejector. Several methods can be used to describe ejector efficiency, and this study applies the definition described by Elbel and Hrnjak (2008), which relates the actual work rate recovered by the ejector $P_{rec} = \dot{m}_0(h_{0,is\to p_8} - h_0)$ to the maximum work rate recovery $P_{rec,max}$:

$$\eta_{ejec} = \frac{P_{rec}}{P_{rec,max}} = \frac{\dot{m}_0\left(h_{0,is\to p_8} - h_0\right)}{\dot{m}_7\left(h_7 - h_{7,is\to p_8}\right)}, \tag{4}$$

where $h_{0,is\to p_8}$ and $h_{7,is\to p_8}$ are the enthalpies obtained by isentropic processes from point 0 and 7, respectively, to the ejector outlet pressure (p_8). The steady-state mass flows used in this definition are related through the 1st law of thermodynamics, e.g. by defining a control volume around both the ejector and the receiver:

$$\dot{m}_7 h_7 + \dot{m}_0 h_0 = \dot{m}_7 h_1 + \dot{m}_0 h_9, \tag{5}$$

and a control volume around the ejector:

$$\dot{m}_7 h_7 + \dot{m}_0 h_0 = \dot{m}_8 h_8, \tag{6}$$

where $\dot{m}_8 = \dot{m}_7 + \dot{m}_0$, i.e., neglecting heat loss and changes in potential and kinetic energies. The ejector efficiency for a given design case, $\mathbf{X}$, with an ejector outlet pressure, p_8, is calculated by creating a custom made function $\eta_{ejec,\mathbf{X}} = g(p_8, \mathbf{X})$ in MATLAB release 2018a (MathWorks, 2018). In the

present work it is assumed that the real ejector efficiency (η_{ejec}) is known, which means that the pressure p_8 can be found by solving:

$$\eta_{\text{ejec}} - g(p_8, \mathbf{X}) = 0, \tag{7}$$

using the built-in MATLAB function fzero, which combines bisection, secant, and inverse quadratic interpolation methods.

Ejector efficiencies up to 34 % are modelled in the sensitivity study, while a 25 % ejector efficiency is used as base case (see Table 2). This is based on the ejector study of CO_2 heat pumps by Banasiak et al. (2012), who measured experimental ejector efficiencies in the range 23 % to 31 %, and simulated values of up to 34 %. Ejector technology can also be applied in R410A systems, e.g. as studied by Pottker and Hrnjak (2015), who measured ejector efficiency between 12 % and 20 %.

2.1.2 Compressor Performance Modelling

Compressor performance is calculated using isentropic efficiency, which is defined as:

$$\eta_{\text{comp}} = \frac{P_{\text{comp,is}}}{P_{\text{comp}}} = \frac{h_{3,\text{is}} - h_2}{h_3 - h_2}, \tag{8}$$

where $P_{\text{comp,is}}$ is an isentropic compression process from point 2 to pressure p_3. Figure 5 shows efficiency and operating range data for the CO_2-based Dorin CD1000H compressor, which is based on a vendor model for the Dorin CD1000H compressor (Wolf, 2015), where efficiency is calculated from compressor inlet pressure (p_2), inlet temperature (T_2), and outlet pressure (p_3), as explained in detail by Brodal et al. (2018). This compressor operates with efficiencies between 67 % and 71 % for $T_{\text{evap@p}_2} = 0$ °C in a transcritical cycle (i.e. over p_{crit}), even if $T_{\text{evap@p}_2}$ is shifted a few degrees, e.g. by an ejector. Figure 6 shows the isentropic efficiency for six additional compressors, and was calculated using data obtained from online software from Bitzer and GEA.

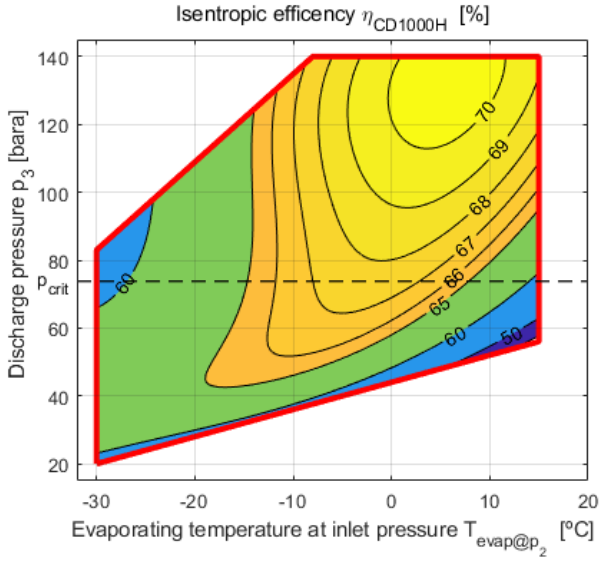

Figure 5. Isentropic efficiency of the CO_2-based CD1000H compressor, assuming 10 K superheating.

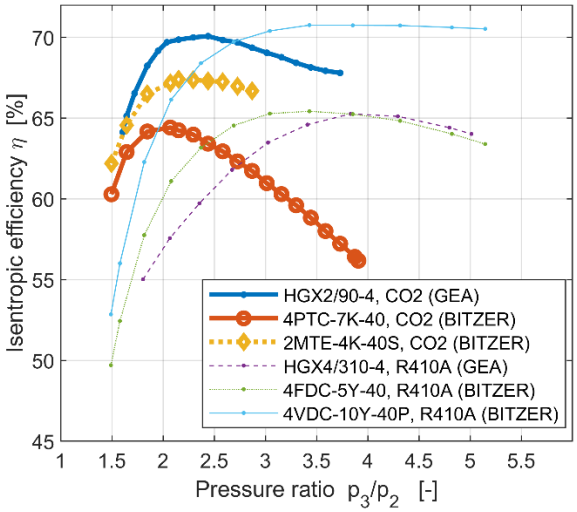

Figure 6. Isentropic efficiency for six different compressors with 10 K superheating and an evaporating temperature at inlet pressure $T_{evap@p_2} = 0$ °C.

Figure 5 and 6 show that the R410A-based 4VDC-10Y-40P compressor from Bitzer has a maximum isentropic efficiency of 71 %, which is almost identical to the CO_2-based CD1000H compressor from Dorin and the HGX2/90-4 CO_2 compressor from GEA. Even the larger CO_2-based CD4000H compressor, is not more efficient than the 4VDC-10Y-40P compressor. During the course of this study we have found that all of the CO_2 compressors operate with pressure ratios between 2.2 – 2.7 in systems without an ejector and between 2.1 – 2.6 in systems with an ejector (see Figure 9). At these pressure ratios the HGX2/90-4 CO_2 (GEA) compressor is operating at almost constant isentropic efficiency between 69 – 70 %, as illustrated by Figure 6. The R410A systems operate with pressure ratios typically between 3 – 5, where the 4VDC-10Y-40P compressor from Bitzer operates with isentropic efficiency between 70 – 71 %. That is, these compressors operate with efficiencies close to their maximum, which reflects the fact that they are designed for such operating conditions. Since these compressors efficiencies are almost constant for the systems investigated here, it was decided to model the compressors with constant isentropic efficiency in order to reduce modelling complexity and therefore making the results more general and easier to apply by others. The isentropic efficiency assumption is tested by presenting results obtained using the Dorin CD1000H compressor efficiency, which is also calculated with a more sophisticated compressor model.

Based on the compressor performances shown in Figures 5 and 6, this study uses 70 % isentropic compressor efficiency as the base case for both CO_2 and R410A compressors, and between 55 % and 75 % in the sensitivity studies (see Table 2).

2.1.3 Design Alternatives

Figure 1 illustrates a heat pump with three gas coolers connected in series “ABC”, but systems with two coolers are also possible, i.e. “AB” and “BC”. ABC is used as the basis for all work, since three coolers allow the most efficient use of heat (Stene, 2005). These systems are also modelled with an ejector and are then named “ABC + ejector”, “AB + ejector” and “BC + ejector”. Heat pump AB and BC are modelled with one less input parameter than described in Eq. (1) since $h_4 = h_3$ in AB and $h_6 = h_5$ in BC. Modelling systems modified with an ejector increases the number of input parameters by one, i.e. the ejector efficiency η_{ejec}.

2.2 Model Optimization, Variables and Constraints

The system model has 14 design parameters ($\mathbf{X}$). The large number makes it difficult to analyze the system directly, for example, finding an optimum set of exchanger sizes, or determining the refrigerant which offers the lowest power consumption for a given operating case. The approach here is, therefore, to reduce the problem size through optimization. For example, instead of

analyzing how the process is affected by p_3, it is assumed that p_3 is always optimal with respect to energy consumption, which is the case if the set pressure of the throttling valve is operated by an intelligent control system. Similarly, if the exchangers are designed for a particular set of operating conditions, it can be assumed that the exchanger sizes to some extent can be optimized for the task. That is, T_2, h_4, h_5, h_6 are optimized for each case and not directly explored in the sensitivity studies. In this approach the temperature pinch becomes the most important factor describing the heat exchanger sizes.

2.2.1 Optimization Parameters and Constraints

The 14 parameters in $\mathbf{X}$ can be divided into two categories:

- Optimized variables ($\mathbf{Z}$) related to process control (p_3) and heat exchanger design (T_2, h_4, h_5, h_6).
- Variables ($\mathbf{Y}$) contain the other operating conditions and equipment variables ($\mathbf{Y} = \mathbf{X} - \mathbf{Z}$).

A list of the optimization parameters, and the constraints applied, are shown in Table 1.

Table 1. Optimized parameters and constraints for heat pump ABC. Heat pump AB and BC are modelled with one less parameter since these systems only have two gas coolers, $h_4 = h_3$ and $h_6 = h_5$ respectively.

Parameters (Z)	Constraints
p_3	$p_3 \geq p_2$
T_2	$T_6 - T_{\text{min,pinch}} \geq T_2 \geq T_1$
h_4	$h_3 \geq h_4 \geq h_5$
h_5	$h_4 \geq h_5 \geq h_6$
h_6	$h_5 \geq h_6 \geq h_7$
	$T_7 \geq T_1 + T_{\text{min,pinch}}$
	$T_{\text{pinch}} \geq T_{\text{min,pinch}}$

The objective function, in the minimization problem, is therefore defined as:

$$\min\{-\text{COP}(\boldsymbol{Z})\}, \text{ for given } \mathbf{Y}, \tag{9}$$

which has $n = 11$ constraints (the inequalities are shown in Table 1). In particular, the requirement $T_{\text{pinch}} \geq T_{\text{min,pinch}}$ complicates the optimization problem, because all the optimization parameters are directly related to pinch temperatures. However, a direct optimization approach is possible by implementing all the constraints in a penalty function:

$$q(\mathbf{Z}) = -\text{COP}(\mathbf{Z}) + \sum_{i=1}^{n} k_i \cdot [\max(0, g_i(\mathbf{X}))]^2, \tag{10}$$

where k_i are penalty factors and g_i constraints function listed in Table 1. The pinch constraint is e.g. defined as:

$$g_{11}(\mathbf{X}) = T_{\text{min,pinch}} - T_{\text{pinch}}(\mathbf{X}). \tag{11}$$

2.2.2 Optimization Algorithm

There are multiple optimization algorithms available in MATLAB, and the current code optimizes the processes with a hybrid method combining multiple fminsearch and genetic algorithm (ga) searches (Eiksund et al., 2018). Fminsearch is a deterministic solver based on the Nelder-Mead simplex algorithm which can find a local minimum with a few function evaluations (Nelder and Mead, 1965), while ga is a stochastic optimization technique suitable to compute the global minimum (Goldberg, 1989).

2.2.3 Selection of Temperature Pinch Constraints

Although pinch constraints are not generally reported in earlier studies, Stene (2005) presents experimental data sets for a similar integrated CO_2 heat pump, from which an estimate of the pinch temperature can be determined.

Figure 7 shows experimental data from Stene (2005) together with simulated data obtained with the optimization routine developed in this study, where the minimum temperature pinch is adjusted to reproduce the experimentally measured COP at T_{d}=70 °C, and using $\bar{T}_{\mathrm{evap}} = -5$ °C, $\eta_{\mathrm{comp}} = 54$ % and $T_{\mathrm{a}} = 6.5$ °C. Based on Figure 7, a 2 K minimum pinch temperature ($T_{\mathrm{min,pinch}}$) is used as base case, and minimum pinch range from 1 to 10 K is used in the sensitivity study (see Table 2).

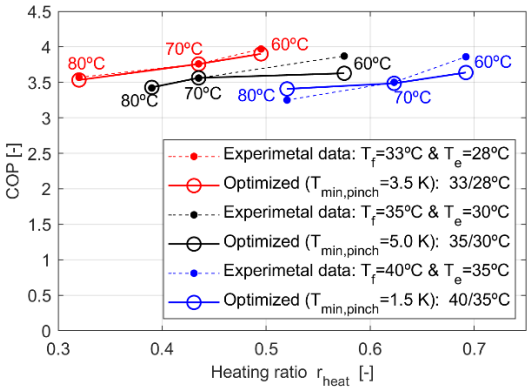

Figure 7. COP for T_d =60°C, 70°C, 80°C as reported by Stene (2005), and modelled COP values where $T_{min,pinch}$ is adjusted to reproduce the experimentally measured COP at T_d=70°C.

2.3 Summary of Design Variables – Study Range and the Base Case

Feedwater temperature (T_{a}) is studied in the range from 2 to 30 °C, and the average temperature reported by Stene (2005), at 6.5 °C, is used as a base case. Heat pumps operate differently with varying space and water heating loads, a large range in heating ratios (r_{heat}) has been set to describe COP in both DHW mode (r_{heat}=0) and space heating mode (r_{heat}=∞). This article only studies cases where the average evaporation temperature $\bar{T}_{\mathrm{evap}} = 0$ °C, space heating is operating with $T_{\mathrm{f}} = 35$ °C and $T_{\mathrm{e}} = 30$ °C, and the feedwater is warmed to T_{d} = 70 °C. The other design variables, which are listed in Table 2, are varied in the sensitivity study.

Table 2. Design and case variables used in sensitivity tests.

Parameter (Y)	**Study range**	**Base case**
Refrigerant (R_{refrig})	CO_2 and R410A	-
Space to water heating ratio (r_{heat})	0 to 10	-
Feedwater temperature (T_{a})	2 to 30 °C	6.5 °C
Minimum pinch temperature ($T_{\mathrm{min,pinch}}$)	1 to 10 K	2.0 K
Pressure drop in heat exchangers (Δp_{ex})	0 to 0.5 bar	0.2 bar
Compressor efficiency (η_{comp})	55 to 75 %	70 %
Ejector efficiency (η_{ejec})	17 to 34 %	25 %

3 Results

Modelled integrated heat pump data is first presented for different CO_2-based systems. The base case with three gas coolers (ABC), is then modelled in a sensitivity study comparing CO_2 and R410A.

3.1 System Design for CO_2-Based Heat Pumps

Figure 8 shows how the COP varies for different designs with three gas coolers (ABC) and other systems with two (AB and BC). All designs are modelled with and without an ejector, using the base case parameters defined in Table 2. Results based on the CD1000H compressor vendor efficiency are also presented for the ABC system. Figure 9 illustrates how the optimized pressures and temperatures vary for two cases (with and without an ejector). Note that the optimal temperatures T_4 and T_5 are not unique if r_{heat}< 0.1, i.e. where space heating can be integrated with $T_{\mathrm{pinch}} > T_{\mathrm{min,pinch}}$.

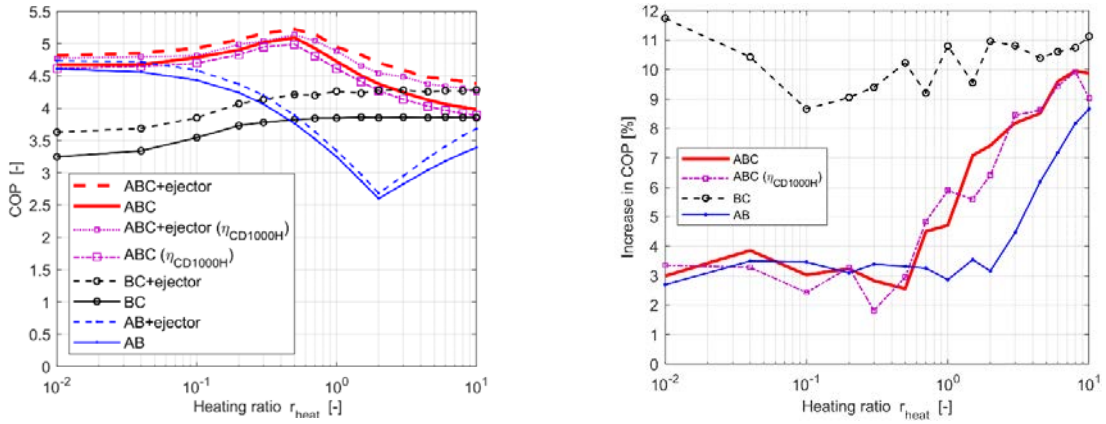

Figure 8. Optimized COP for different designs using CO_2 (left), and the percentage increase in COP with ejector (right).

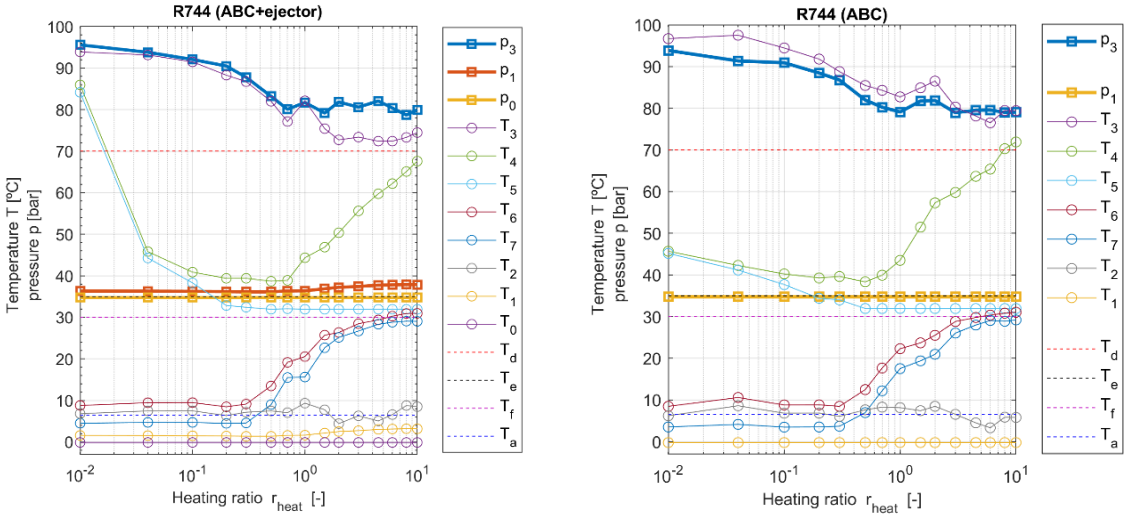

Figure 9. Process parameters (optimized) for CO_2-based designs with an ejector (left) and without (right).

3.2 Sensitivity Study Comparing CO_2 and R410A

The impact of pinch temperature and feedwater temperature on COP is illustrated in Figure 10.

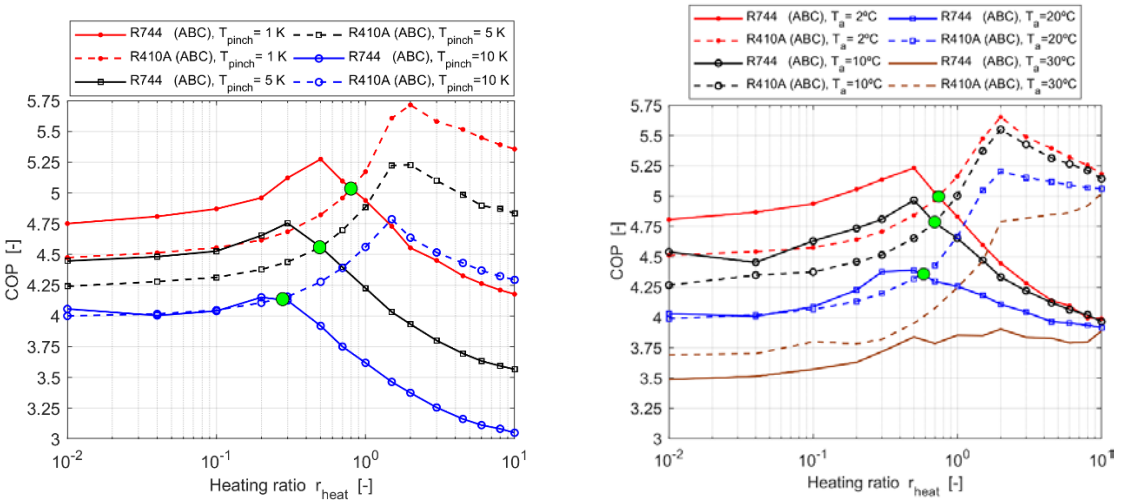

Figure 10. COP for different pinch temperatures (left) and feedwater temperatures (right). The green circles indicate where R744 and R410A curves cross.

The impact of compressor performance, pressure drops in heat exchangers and ejector performance is illustrated in Figure 11. Table 3 provides a summary of the increase in COP for the different ejector efficiencies scenarios from Figure 8 and 11.

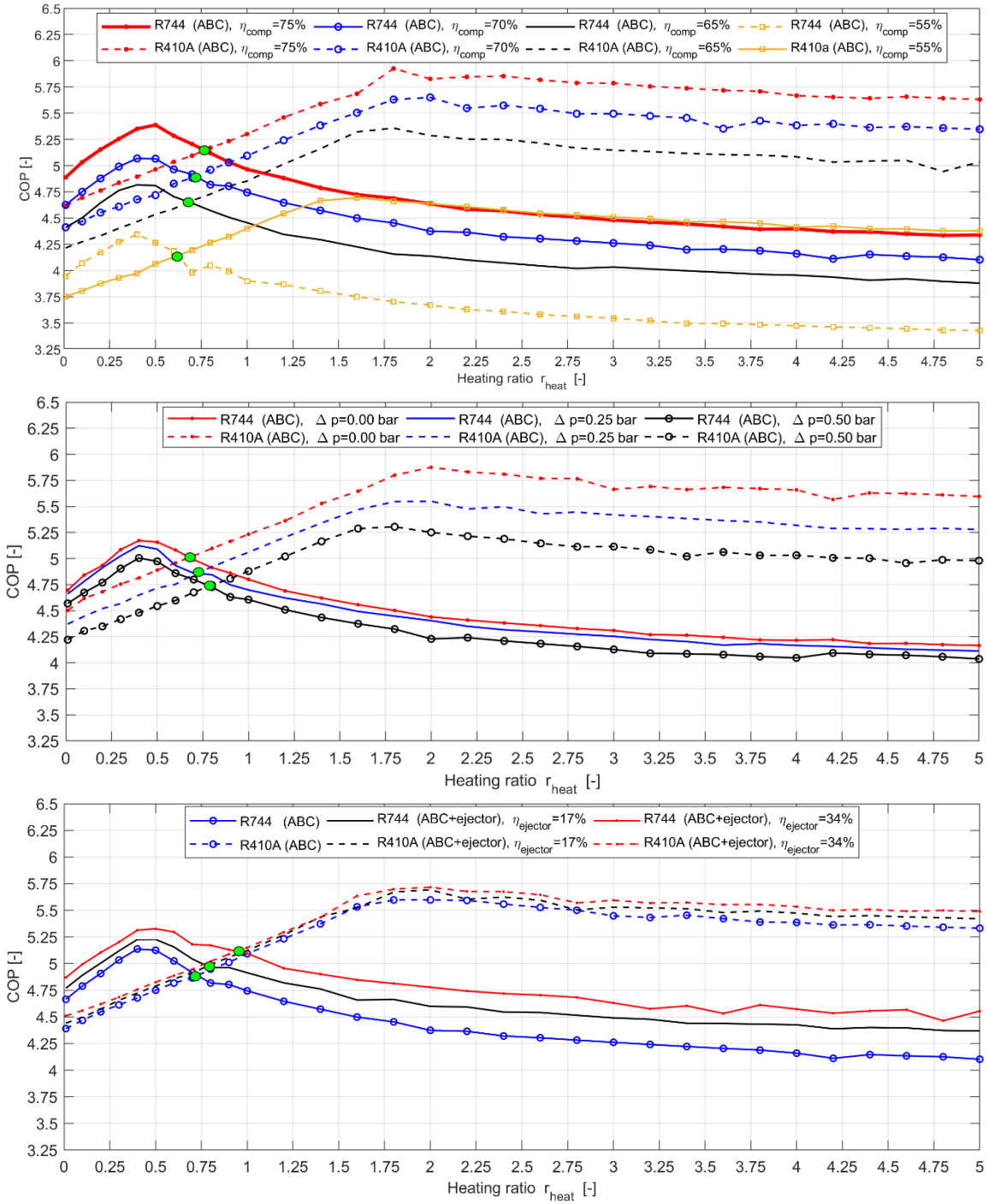

Figure 11. COP using different compressor efficiencies (top), pressure drops (middle) and ejector efficiencies (bottom). The green circles indicate where R744 and R410A curves cross.

Table 3. COP for different heating ratios r_{heat} and ejector efficiencies scenarios.

r_{heat} [-]	COP [-] (Gain in COP by inclusion of an ejector [%])						
	R744 ABC	**R410A ABC**	**R744 ABC + ejector 17 %**	**R744 ABC + ejector 25 %**	**R744 ABC + ejector 34 %**	**R410A ABC + ejector 17 %**	**R410A ABC + ejector 34 %**
0.0	4.67	4.39	4.77 (2.2 %)	4.82 (3.0 %)	4.87 (4.4 %)	4.44 (1.2 %)	4.51 (2.7 %)
1.0	4.74	5.09	4.91 (3.6 %)	4.95 (4.7 %)	5.10 (7.4 %)	5.12 (0.6 %)	5.15 (1.2 %)
5.0	4.10	5.33	4.37 (6.4 %)	4.49 (8.8 %)	4.56 (11.0 %)	5.42 (1.7 %)	5.49 (2.9 %)

4 Discussion

The main focus of the article is to investigate performance of CO_2-based integrated heat pumps, and compare them with systems based on conventional R410A-based systems.

4.1 Modelling Basis

Performance of integrated heat pumps are calculated in MATLAB by combining models of the main components in the system, i.e., heat exchangers, compressor and ejector. The compressor outlet pressure is optimized for the operative conditions in each case. The heat pump model is based on multiple variables optimization algorithms (ga and fminsearch), since also the duty of each exchanger is optimized.

4.1.1 Exchangers

The approach in this article is based on a model using the minimum allowed temperature approach as an input, assuming that the heat exchanger design is optimized for the given operating condition. Earlier literature is influenced by heat exchangers design, either by fixed exchangers in experimental setups, or by applying heat exchangers models with many input parameters in theoretical studies. These heat exchanger parameters increase the complexity in previous work, and make it difficult to identify the conditions where e.g. CO_2 outperform R410A-based systems.

4.1.2 Compressor

In this study, compressors are either modelled with a constant efficiency, or the Dorin CD1000H (CO_2) compressor vendor model. The difference between the two approaches is small, as illustrated by almost parallel lines in Figure 8. Figure 9 shows that the outlet pressure is always between 78 and 95 bar, which corresponds to an isentropic compressor efficiency between 67 and 69 % (see Figure 5). As shown in Figure 6, the CO_2-based GEA HGX2/90-4 compressor typically operates with an isentropic efficiency between 69 – 70 %, and the Bitzer 4VDC-10Y-40P (R410A) compressor between 70 – 71 %. That is, both the most efficient R410A and CO_2 compressors identified in this study are modelled relatively accurate by a 70 % isentropic efficiency.

4.2 Impact of System Design

Figure 8 presents results that show the improvements going from two gas coolers (AB or BC) to three (ABC) are significant, which support the selection of the ABC design as the base case for this study.

4.2.1 The Impact of Compressor Efficiency

Figure 11 shows that CO_2 systems benefit more by having a compressor with a high isentropic efficiency, e.g. if both systems have a compressor with a 55 % efficiency, the CO_2 unit is more efficient for heating ratios $r_{\text{heat}} \leq 0.6$, while the CO_2 unit is more efficient for $r_{\text{heat}} \leq 0.8$ if the units have 75 % isentropic compressor efficiency. Differences in real equipment performance is discussed in Section 4.3.4.

4.2.2 Conventional Expansion Valve vs. Ejector

Figure 8 shows the ejector gain, compared to conventional expansion valve systems, in CO_2-based systems with 25 % ejector efficiency. COP increases from 3 % (in DHW mode) to 10 % (in space heating mode), i.e., a large gain is obtained in cases where CO_2 is inefficient compared to R410A. Table 3 shows that the increase in COP is in the range 3.6 – 7.4 % for the CO_2 cases with r_{heat} = 1.0, where CO_2 and R410A-based systems have similar COP. The results in Table 3 compare well with the findings of Banasiak et al. (2012) showing that an ejector could increase COP with 8 %. Table 3 also shows that there is little to gain by including an ejector in the R410A cycle, less than 3 % gain in COP. R410A-based integrated heat pumps are therefore unlikely to be designed with an ejector, which is supported by Minetto et al. (2016).

The ejector gain can be significant for systems with two gas coolers. Figure 8 shows that the gain in COP can be as large as 12 % for the scenarios studied here, but the gain can be bigger. For example, Minetto et al. (2016) obtained a gain close to 20 % for a similar gas cooler setup as "AB", since the ejector process benefited from higher gas cooler outlet CO_2 temperatures and ejector efficiencies.

4.2.3 Electrical Heating

The operating pressures are always within the CD1000H compressor range, and the optimized results show that it is always more efficient to deliver all the heat using the heat pump, i.e. using zero auxiliary heating.

4.3 Conventional Refrigerants vs. CO_2

The discussion presented below is based on the assumption that COP is compared based on equal premises, i.e. the same equipment performance parameters and case values.

4.3.1 The Impact of Heat Demand

The sensitivity study shows that CO_2-based systems typically obtain the best COP for heat demand ratios around $r_{\text{heat}} \approx 0.5$, which are typical in modern energy-efficient buildings. CO_2 can be the best alternative for ratios up to 1.0 for systems where ejectors are used in combination with efficient compressors, cold feedwater, and large exchangers giving tight pinch temperatures and high pressure drops.

Figure 8 – 11 show that process efficiency can be improved if low temperature space heating is added to DHW heating. The optimal r_{heat} for CO_2 is typically between 0.35 and 0.55, depending on feedwater temperature, pinch temperature and pressure drop in heat exchangers. For R410A systems, the optimal r_{heat} is between 1.7 and 2.0. In CO_2-based systems, the COP is reduced significantly in the space heating mode where the temperature in the gas coolers no longer matches the heating demand profiles.

Figure 10 and 11 show that CO_2-based systems outperform established R410A systems in DHW heating mode, or if the ratio between space and water heating is low. COP is up to 10 % higher for CO_2 systems in DHW heating mode. This is smaller than the 20 % suggested by Stene and Alonso (2016), however, this study referred to conventional R410A systems using auxiliary heating to supply high DHW temperature, as discussed by Blanco et al. (2012), and was also based on real equipment performance. The designs studied here (see section 2.1) do not need auxiliary heating, and all the optimized results presented have zero auxiliary heating.

4.3.2 The Impact of Feedwater Temperature

Figure 10 shows that COP is reduced as feedwater temperature increases. COP is reduced with 6 % when it increases from 2 °C to 10 °C in the DHW heating mode processes. If it increases from 20 °C to 30 °C, the reductions in COP are 8 % and 14 % for R410A and CO_2, respectively. For feedwater temperatures above 30 °C, R410A-based systems are always best. Figure 10 also shows that CO_2-based systems outperform conventional R410A units if the ratio between space and water heating is low and the feedwater is below 20 °C. Hence, CO_2-based systems are an interesting technology for low-energy buildings in northern Europe.

In conventional transcritical heat pumps it is normal to expect that the optimum gas cooler pressure (p_3) increases with the outlet temperature of the gas cooler (T_6). However, Figure 8 and 9 show that this is not always the case for integrated heat pumps, where the relationship between p_3 and T_6 depends on the heating ratio r_{heat}. That is, T_6 is reduced if r_{heat} is reduced due to the increased low temperature heating demand created by the cold tap water entering at 6.5 °C, while it is sometimes necessary to increase p_3 to cover the high temperature heating demand related to production of 70 °C hot water.

4.3.3 The Impact of Pressure Drop

Figure 11 shows that COP is reduced with increased pressure drop, and that pressure drop has a greater impact on R410A-based systems which operate at lower pressure than CO_2. For a DHW heating mode process with R410A, COP is reduced with 6 % if the pressure drop increases from 0 to 0.5 bar. In a CO_2 process, the corresponding reduction is less than 3 %.

4.3.4 The Impact of Temperature Pinch

In this article it is assumed that the heat exchangers are designed/sized to obtain a given minimum temperature pinch for a given operating condition. Figure 10 shows that tight pinch temperatures are more important for CO_2 processes than R410A, and that R410A is more efficient than CO_2 if the exchangers are designed for temperature pinch above 10 K. In the DHW heating mode, COP is reduced with approximately 6 % for both CO_2 and R410A processes if the pinch increases from 1 K to 5 K. If the pinch increases from 5 K to 10 K, COP is reduced with 5 % in R410A processes and 9 % in CO_2 processes. However, note that real systems with fixed heat exchangers will not operate at constant temperature pinches when operating with off-design conditions.

Because the approach temperature used in the gas cooler for CO_2 and the condenser for R410A implies different cost and performance impacts for each refrigerant, it is important to study the sensitivity of this assumption. To support this, system performance for both CO_2 and R410A was studied at temperature approaches of 1, 2 and 10 K. Figure 10 shows that COP for both refrigerants is reduced with 1 – 2 % for each degree Celsius the minimum temperature pinch is raised. However, the results presented in this article compare systems with large gas coolers, since they are assumed to operate with a relatively small minimum temperature pinch of 2.0 K. Hence, the impact of minimum temperature pinch variations on COP is small for the results presented in this study. Based on data from Figure 10, other heat exchanger parameters could be studied in the future by, e.g. by calculating realistic temperature pinches from fixed heat exchangers models as discussed by Chen (2016), or from models provided by heat exchanger vendors.

4.4 Other Considerations

The assumption that systems with different refrigerants have the same equipment performance parameters are simplifications discussed below.

4.4.1 Differences in Real Equipment Performance

The process depends on the equipment, which again depends on properties of the refrigerant. For example, CO_2 exchangers and other equipment have to be designed for higher pressures, but CO_2 also has some advantages over R410A, like better heat transfer properties (Park and Hrnjak, 2007). In addition, CO_2 has low GWP, which favors CO_2 when comparing the total equivalent warming impact (TEWI).

Stene and Alonso (2016) argue that CO_2 processes also benefit from high compressor efficiencies due to low pressure ratio, in this study however, only a small difference in compressor performance is found between the most efficient R410A and CO_2 compressors as illustrated by Figure 6. The 4VDC-10Y-40P (R410A) compressor from Bitzer, for example, was identified to operate at a nearly identical isentropic efficiency as the CD1000H compressor. However, the CO_2 systems need compressors with less displacement due to the high inlet density.

CO_2 heat pumps can typically be constructed with a lower pressure drop than in R410A heat pumps (Stene and Alonso, 2016), however, since the pressure drop has only a small impact on the CO_2 process, CO_2 systems require little power input to circulate the working fluid. Larger pressure drop generates higher velocities and better heat transfer in the exchangers, which in turn, can overcome the thermodynamic losses directly related to the pressure drop. CO_2 systems can therefore be designed with large pressure drop in the exchangers to obtain better COP. The difference in heat

transfer in equally sized exchanges can, to some extent, be compensated by comparing R410A with CO_2 systems that have a smaller temperature pinch.

It has been claimed that the efficiency of CO_2 ejectors is generally in the range of 20 – 30 %, while the efficiency of ejectors for low-pressure refrigerants such as R410A typically is less than 20 % (Elbel and Lawrence, 2016). Table 3 also shows that there is little to gain by including an ejector in the R410A cycle. Due to the small improvement, less than 3 % gain in COP, R410A-based integrated heat pumps are unlikely to be designed with an ejector. This is supported by Minetto et al. (2016) who compared reversible heat pumps based on CO_2 and R410A, but only included ejectors in the CO_2 systems.

Figure 10 shows that if both the CO_2 and R410A systems have a 1 K temperature pinch, the CO_2 heat pump is most efficient for $r_{\text{heat}} \leq 0.8$. However, because low pinch temperatures are both more important and easier to achieve in CO_2-based systems, it is likely that such systems would be designed for a tighter approach than an equivalent R410A system, therefore, the performance advantage illustrated by this work could be considered conservative. For example, if the CO_2 systems have a 1 K temperature pinch, while the R410A system have a 5 K temperature pinch, the CO_2 heat pump is the most efficient for $r_{\text{heat}} \leq 1.0$. As mentioned in the introduction, the use of high GWP refrigerants like R410A will be reduced through regulations. The results show that CO_2 is an excellent replacement refrigerant for small heating ratios r_{heat}. However, since CO_2 systems are inefficient compared to R410A for r_{heat} larger than 1.0, it is important to investigate other low GWP replacement refrigerants for such heating scenarios.

4.4.2 The Impact of Variations in Heat Demand

The heat demand will typically variate both on a daily and a yearly basis, which means that the heat pump can be expected to sometimes operate in both pure space heating and DHW mode. Figure 8 shows that it is important to include an ejector if the system is running in DHW mode. If a system only switches between two modes, $r_{\text{heat}} = 0$ and $r_{\text{heat}} = 5$, Figure 11 shows that a heat pump must generate more than 81 % of the heat in the $r_{\text{heat}} = 0$ mode before CO_2 is the best alternative. If an ejector is used, CO_2 is best if the system produces more than 72 % of the heat in the $r_{\text{heat}} = 0$ mode. However, such variations in heat demand are modelled more realistic with a system having fixed heat exchangers.

5 Conclusions

This study presents integrated heat pump performance at a variety of operating conditions, using the assumption that the design is optimized for those conditions. The modelling work is based on a minimum allowed temperature approach in the heat exchangers and realistic compressor efficiency data. Multivariable optimization techniques based on temperature pinches have earlier been used in sensitivity studies for LNG cascade processes, but this is a new approach when applied to the modelling of integrated heat pumps. This approach enables a better understanding of the impact of important performance factors than presented in previous studies of integrated heat pumps.

The systems modelled here show that CO_2 can outperform R410A when the ratio between space and water heating is lower than 0.6 – 1.0, and the feedwater is colder than 20 °C (for example in Northern Europe) and the exchanger designs have tight pinch temperatures below 10 K. However, it is believed that these are conservative estimates with respect to the CO_2 heat pumps, since differences in real equipment performance are not accounted for, as explained in the discussion. Efficient compressors and the use of ejector also benefits CO_2-based systems. However, the sensitivity study shows that R410A processes always can be assumed to be more efficient for space to DHW heating ratios above 1.

The sensitivity studies presented in this article allow the comparison of R410A and CO_2 based systems where process parameters such as compressor efficiency vary with the refrigerant used. For example, Figure 11 shows CO_2 to have higher COP for space heating to water heating ratios less than 0.7 when the compressor efficiency for both CO_2 and R410A is 70 %, whereas if the efficiency of the R410A compressor is 65 % a CO_2 based system has higher COP up to ratios of around 0.9. Future work is needed to understand how differences in CO_2 and R410A equipment performance will affect the COP.

The optimization model is also used to investigate the COP gain made by introducing an ejector. Modelling of integrated heat pumps with multiple gas coolers and an ejector has not been studied in detail before. Results computed in this article show that the gain in COP is small (less than 3%) for R410A. For CO_2, the ejector gain can be up to 11 %, and the gain in space heating mode is more than double the gain in DHW mode. Hence, a CO_2-based integrated heat pump with an ejector is a recommended heating system for modern, well insulated, low-energy buildings.

REFERENCES

Arpagaus, C., Bless, F., Schiffmann, J., Bertsch, S.S., 2016. Multi-temperature heat pumps: A literature review. International Journal of Refrigeration 69, 437-465.

Banasiak, K., Hafner, A., Andresen, T., 2012. Experimental and numerical investigation of the influence of the two-phase ejector geometry on the performance of the R744 heat pump. International Journal of Refrigeration 35(6), 1617-1625.

Banasiak, K., Hafner, A., Kriezi, E.E., Madsen, K.B., Birkelund, M., Fredslund, K., Olsson, R., 2015. Development and performance mapping of a multi-ejector expansion work recovery pack for R744 vapour compression units. International Journal of Refrigeration 57, 265-276.

Bell, I.H., Wronski, J., Quoilin, S., Lemort, V., 2014. Pure and Pseudo-pure Fluid Thermophysical Property Evaluation and the Open-Source Thermophysical Property Library CoolProp. Industrial & Engineering Chemistry Research 53(6), 2498-2508.

Bitzer. Online compressor software <https://www.bitzer.de/websoftware/> Accesed April 2018.

Blanco, D.L., Nagano, K., Morimoto, M., 2012. Steady state vapor compression refrigeration cycle simulation for a monovalent inverter-driven water-to-water heat pump with a desuperheater for low energy houses. International Journal of Refrigeration 35(7), 1833-1847.

Boccardi, G., Botticella, F., Lillo, G., Mastrullo, R., Mauro, A.W., Trinchieri, R., 2017. Experimental investigation on the performance of a transcritical CO_2 heat pump with multi-ejector expansion system. International Journal of Refrigeration 82, 389-400.

Brodal, E., Jackson, S., Eiksund, O., 2018. Transient model of an RSW system with CO_2 refrigeration – A study of overall performance. International Journal of Refrigeration 86, 344-355.

Byrne, P., Miriel, J., Lenat, Y., 2009. Design and simulation of a heat pump for simultaneous heating and cooling using HFC or CO_2 as a working fluid. International Journal of Refrigeration 32(7), 1711-1723.

Chen, Y.-G., 2016. Pinch point analysis and design considerations of CO_2 gas cooler for heat pump water heaters. International Journal of Refrigeration 69, 136-146.

Ding, H., Sun, H., Sun, S., Chen, C., 2017. Analysis and optimisation of a mixed fluid cascade (MFC) process. Cryogenics 83, 35-49.

Eiksund, O., Brodal, E., Jackson, S., 2018. Optimization of Pure-Component LNG Cascade Processes with Heat Integration. Energies 11(1), 202.

Elbel, S., Hrnjak, P., 2008. Experimental validation of a prototype ejector designed to reduce throttling losses encountered in transcritical R744 system operation. International Journal of Refrigeration 31(3), 411-422.

Elbel, S., Lawrence, N., 2016. Review of recent developments in advanced ejector technology. International Journal of Refrigeration 62, 1-18.

Elmegaard, B., Ommen, T.S., Markussen, M., Iversen, J., 2016. Integration of space heating and hot water supply in low temperature district heating. Energy and Buildings 124, 255-264.
EU, 2014. Regulation No 517/2014 of the European Parliament and of the Council of 16 April 2014 on fluorinated greenhouse gases and repealing Regulation (EC). Official Journal of the European Union(1).
GEA. Online compressor software <https://vap.gea.com> Accesed April 2018.
Goldberg, D.E., 1989. Genetic Algorithms in Search, Optimization and Machine Learning. Addison-Wesley Longman Publishing Co., Inc.
Heinz, A., Martin, K., Rieberer, R., Kotenko, O. (2010). Experimental analysis and simulation of an integrated CO_2 heat pump for low-heating-energy buildings. Sidney, Australia.
Hepbasli, A., Kalinci, Y., 2009. A review of heat pump water heating systems. Renewable and Sustainable Energy Reviews 13(6), 1211-1229.
Lemmon, E.W., 2003. Pseudo-Pure Fluid Equations of State for the Refrigerant Blends R-410A, R-404A, R-507A, and R-407C. International Journal of Thermophysics 24(4), 991-1006.
MATLAB, 2018. The MathWorks Inc.
Minetto, S., Cecchinato, L., Brignoli, R., Marinetti, S., Rossetti, A., 2016. Water-side reversible CO_2 heat pump for residential application. International Journal of Refrigeration 63, 237-250.
Nekså, P., 2002. CO_2 heat pump systems. International Journal of Refrigeration 25(4), 421-427.
Nekså, P., Rekstad, H., Zakeri, G.R., Schiefloe, P.A., 1998. CO_2-heat pump water heater: characteristics, system design and experimental results. International Journal of Refrigeration 21(3), 172-179.
Nelder, J.A., Mead, R., 1965. A Simplex Method for Function Minimization. The Computer Journal 7(4), 308-313.
Nord, N., Schmidt, D., Kallert, A.M., Svendsen, S., 2016. Improved Interfaces for Enabling Integration of Low Temperature and Distributed Heat Sources – Requirements and Examples. CLIMA 2016 - proceedings of the 12th REHVA World, Aalborg University.
Park, C.Y., Hrnjak, P.S., 2007. CO_2 and R410A flow boiling heat transfer, pressure drop, and flow pattern at low temperatures in a horizontal smooth tube. International Journal of Refrigeration 30(1), 166-178.
Pottker, G., Hrnjak, P., 2015. Ejector in R410A vapor compression systems with experimental quantification of two major mechanisms of performance improvement: Work recovery and liquid feeding. International Journal of Refrigeration 50, 184-192.
Richter, M.R., Song, S.M., Yin, J.M., Kim, M.H., Bullard, C.W., Hrnjak, P.S., 2003. Experimental results of transcritical CO_2 heat pump for residential application. Energy 28(10), 1005-1019.
Span, R., Wagner, W., 1996. A New Equation of State for Carbon Dioxide Covering the Fluid Region from the Triple-Point Temperature to 1100 K at Pressures up to 800 MPa. Journal of Physical and Chemical Reference Data 25(6), 1509-1596.
Stene, J., 2005. Residential CO_2 heat pump system for combined space heating and hot water heating. International Journal of Refrigeration 28(8), 1259-1265.
Stene, J., 2007. IEA HPP Annex 32 - Economical heating and cooling systems for low-energy houses State-of-the-art report Norway (SINTEF-EF-TR-A--6506)
Stene, J., 2007. Integrated CO_2 heat pump systems for space heating and hot water heating in low-energy houses and passive houses. International Energy Agency (IEA) Heat Pump Programme – Annex 32 – Workshop in Kyoto, Japan.
Stene, J., Alonso, M.J., 2016. Field Measurements – Heat Pump Systems in NZEB. SINTEF Academic Press.
Wilhelmsen, Ø., Skaugen, G., Jørstad, O., Li, H., 2012. Evaluation of SPUNG and other equations of state for use in carbon capture and storage modelling. Energy Procedia 23, 236-245.
Wolf, S.R.L., 2015. DORIN Software (version 15.07). DORIN,
Yokoyama, R., Shimizu, T., Ito, K., Takemura, K., 2007. Influence of ambient temperatures on performance of a CO_2 heat pump water heating system. Energy 32(4), 388-398.